

Electroreduction of Dipyridamole at Mercury-Coated Platinum Microelectrode

Renata A. de Toledo, Marilza Castilho and Luiz Henrique Mazo*

Instituto de Química de São Carlos, Universidade de São Paulo, CP 780, 13560-970 São Carlos - SP, Brazil

A eletrorredução do Dipiridamol (DIP) foi estudada em solução tampão fosfato 0,10 mol L⁻¹ (pH 3,0) em microeletrodo de platina coberto com mercúrio eletrodepositado (Hg-ME), empregando as técnicas de voltametria cíclica, de varredura linear e polarografia. A similaridade entre o perfil voltamétrico obtido com Hg-ME e as ondas polarográficas sigmoidais com correntes limitadas por difusão é demonstrada. Experimentos com eletrodo de gota pendente de mercúrio (HMDE) foram realizados em paralelo para confirmar os resultados obtidos com Hg-ME, os quais indicaram que a reação de redução ocorre em duas etapas irreversíveis com o consumo de dois elétrons e dois prótons por etapa. A corrente limite de difusão, referente à primeira etapa de redução, permitiu estimar o coeficiente de difusão do DIP como sendo igual a 2,04 x 10⁻⁵ cm² s⁻¹.

The electroreduction of Dipyridamole (DIP) was studied in 0.10 mol L⁻¹ phosphate buffer solution (pH 3.0) on a mercury coated platinum microelectrode (Hg-ME), employing cyclic, linear sweep voltammetry and polarography techniques. The similarity between Hg-ME voltammetric profile and the sigmoidal polarographic waves both with a diffusion limited current is showed. Experiments with a hanging mercury drop electrode (HMDE) were performed in parallel to confirm the results obtained with Hg-ME, which indicated that the reduction occurs in two irreversible steps involving two electrons and two protons each step. The limiting diffusion current, concerning the first step, allows estimating the diffusion coefficient for DIP as being equal to 2.04 x 10⁻⁵ cm² s⁻¹.

Keywords: dipyridamole, electroreduction, mercury-coated platinum microelectrode, voltammetry

Introduction

Dipyridamole (DIP), 2,6-bis(diethanolamino)-4,8-dipiperidinopyrimido-[5,4-d] pyrimidine, was introduced in 1959 as a coronary vasodilator and an antiplatelet drug, and has been quite used until now in medicine for the treatment of several cardiovascular diseases.¹ Its structure, shown in Figure 1, presents a stable hetero-aromatic double ring core, which is responsible for the characteristic UV-Vis absorption and fluorescence of the compound.²

Recent studies in the literature have reported that DIP also exhibits a potent antioxidant activity behaving as an inhibitor of lipid peroxidation initiated both by iron (II) ions³ and by thermolabile azo compounds.⁴ The electrochemical oxidation of DIP has been extensively studied in our laboratory⁵⁻⁷ in order to bring better understanding about its electrochemical reactions.

Moreover, it has been shown that DIP can reduce the drug uptake resistance of the cells due to its inhibition of the P-glycoprotein,⁸ and also causes the suppression of

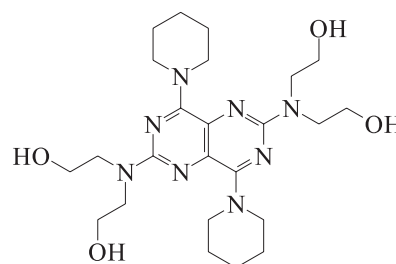


Figure 1. Structure of dipyridamole (DIP).

the growing of some tumor cells.⁹ These applications confer to DIP substantial importance in medicine and pharmaceutical areas, stimulating the study of its action mechanism as well as the development of new analytical methods for DIP quantification in pharmaceutical preparations¹⁰⁻¹² and in biological fluids.¹³⁻¹⁵

There are two works in the literature that deal with the electroreduction of DIP for analytical aims, and no mechanistic study has been carried out until now. In the pioneer work of Tunçel *et al.*,¹⁶ the electroreduction of DIP was studied in phosphate buffer and ethanol 20% (v/v),

* e-mail: lh-mazo@iqsc.usp.br

containing 0.20 mol L⁻¹ KCl as supporting electrolyte. In that experimental conditions, the DC polarograms obtained lead to suppose that the reduction was reversible. Differential pulse polarography was also used among other modes for determination of DIP in commercial tablets.

Later, Zeng *et al.*¹⁷ reported a sensitive voltammetric procedure for trace measurement of DIP, based on its adsorptive accumulation at a hanging mercury drop electrode (HMDE) in 0.05 mol L⁻¹ NaOH, using the adsorptive stripping voltammetric method. The shape of the voltammograms has showed that the reaction is irreversible. The detection limit reached was 1.0 nmol L⁻¹ when the preconcentration time was set to 5 min. Electrolysis experiments revealed that four electrons are transferred per DIP molecule.

In the last few years, the intensive application of microelectrodes (ME) into *in vivo* and *in vitro* studies of many biological molecules and pesticides can be attributed to several interesting features of ME, such as the high mass-transport rates, the reduced capacitive and resistive effects.^{18,19} Mercury microelectrodes (Hg-ME) can be prepared easily using appropriate substrates through electrodeposition of mercury from solutions containing mercurous or mercuric ions.²⁰

Due to the great applicability of DIP in medicine from the common treatment of cardiovascular diseases to other more recent applications, the aim of this work is to study the electroreduction behavior of DIP using a hemispheric mercury coated platinum microelectrode as an alternative of conventional employ of Hg electrodes, minimizing the generation of Hg residues.

Experimental

Chemicals

All reagents used in this work were of analytical grade from Aldrich (dipyridamole), Merck (di-sodiumhydrogen phosphate dihydrate, nitric acid and others) and Sigma (phosphoric acid). Water treated in a Milli-Q system (Millipore) was used to prepare the solutions. All chemicals were used without previous purification.

Preparation of Hg microelectrodes (Hg-ME)

Disk shaped microelectrode of Pt ($\phi = 25 \mu\text{m}$) was constructed in our own research laboratory by insulating Pt microwires into a soft glass capillary tube. For electrical contact, a copper fiber was sealed with the microwire by tin-lead solder. After construction, a surface treatment was carried out with sandpaper and by polishing in a wet cloth

embedded with alumina emulsion of several decreasing granulations until 0.05 μm . The procedure was accompanied by optical microscopy to verify eventual presence of microcrunchs or microbubbles in the borders of the exposed micro-disk. After the polishing procedure, electrochemical characterization of ME was made by application of cyclic voltammetry in K₃Fe(CN)₆ acid solution.

Cronoamperometric technique was used for mercury deposition in solutions containing 0.07 mol L⁻¹ Hg²⁺ ions. Prior to Hg deposition, the solution was bubbled with nitrogen from White Martins (SS grade) for 10 min to remove oxygen, then a constant potential of -1000 mV vs. Ag/AgCl_(s) was applied for 90 seconds to produce a stable mercury hemispheric deposit. Reproducible results could be obtained in order to achieve the best electroanalytical response according to the optimized parameters cited above. The Hg-ME electrode was stable for a day of analysis and the renewed of the hemispheric deposit was quite easy.

Under conditions of large overpotentials the mercury deposition is knew to occur by a polynucleation phenomenon, the final homogeneous deposit being formed by coalescence of the growing microdroplets.^{21,22} The hemispherical deposit radius can be calculated with basis on cronoamperometrical experiments.

Cyclic voltammetry (CV), linear sweep voltammetry (LSV) and polarography

Cyclic and linear sweep voltammograms with mercury coated platinum disk microelectrodes ($\phi = 25 \mu\text{m}$) were recorded with a computerized lab-made system and the currents being measured by a Stanford Research Systems, model SR570 current amplifier. The computerized system uses an IBM compatible personal computer and a lab-made software named AVOLM, wrote in visual basic language.²³ For the experiments with a conventional mercury electrode, a hanging mercury drop electrode (HMDE - A = 0.01 cm²) model MDE150 and a Voltalab model PGZ402 were used.

For the measurements with Hg-ME, a two electrode cell containing a Ag/AgCl_(s) (3.0 mol L⁻¹ KCl) reference electrode and the microelectrode was employed. A conventional three-electrode cell containing a platinum wire counter electrode and a Ag/AgCl_(s) (3.0 mol L⁻¹ KCl) reference electrode was used for the voltammetric application with HMDE and for polarographic experiments.

Tast polarography was carried out in a polarographic analyzer model 384B with a dropping mercury electrode (DME) model 303A, both from EG&G Princeton applied research system.

Solutions of DIP ranging from 10^{-3} to 10^{-4} mol L $^{-1}$ were prepared in 0.10 mol L $^{-1}$ phosphate buffer and purged with purified nitrogen for 5 min prior to the measurements.

Results and Discussion

Calculation of the Hg-ME hemispherical radius

The Hg-ME hemispherical radius was calculated with basis on chronoamperometric experiments. The I vs. time curve was integrated and the resulted charge was used to estimate the approximated hemispherical radius of the mercury deposit. In a typical experiment, the charge obtained was 6.20×10^{-5} A s $^{-1}$, which corresponds to a 1.31×10^{-3} cm electrode radius.

Analysis of the voltammetric profile using Hg-ME

The voltammetric profile of DIP electroreduction using Hg-ME is shown in Figure 2 (I). The observed landings are indicative that, at sufficient cathodic potentials after each reduction waves, the current is limited by diffusion of DIP species to the ME surface. The Tast polarogram (Figure 2 (II)) presents evident polarographic maxima for the two reduction steps, which can be related to adsorption of

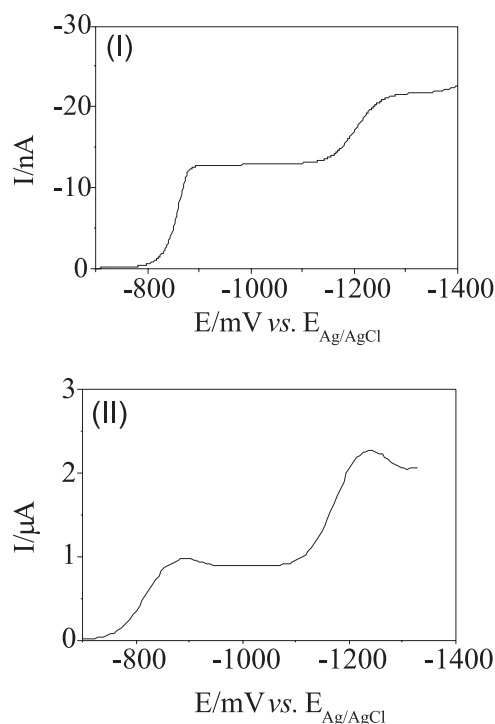


Figure 2. (I) LSV curve for DIP 0.50 mmol L $^{-1}$ in 0.10 mol L $^{-1}$ phosphate buffer solution (pH 3.0), using a Hg-ME. $\nu = 10$ mV s $^{-1}$. (II) DC $_T$ polarogram for DIP 0.50 mmol L $^{-1}$ in 0.10 mol L $^{-1}$ phosphate buffer solution (pH 3.0), using a DME electrode. $\nu = 10$ mV s $^{-1}$. drop time = 0.5 s.

electroactive species on the electrode surface. The same surface accumulation can be responsible for the enhanced in the LSV current observed for the first step.

Effect of scan rate on voltammetric profiles

The voltammetric profiles were registered over the range of scan rate investigated with Hg-ME, and are presented in Figure 3. At low scan rates (Figure 3(I)), the voltammograms show sigmoidal profiles and well-defined limiting currents, which are characteristic of microelectrode response. This steady-state response arises from an increased mass transport due to nonlinear diffusion at electrodes of these dimensions. On the other hand, at high scan rates (Figure 3(II)), the voltammograms begin to show conventional electrode voltammetric responses.

The electrochemical parameters for DIP electroreduction are presented in Table 1 for both waves, including half-wave potential ($E_{1/2}$), diffusion current (I_d), angular coefficient (θ) obtained from $\log(I_d - I)/I$ vs. E curves and $n\alpha$ values calculated from the angular coefficient ($\theta = 59/n\alpha$) at different scan rates. The electrochemical parameters (Table 1) are compatible with an irreversible electrode reaction, since $E_{1/2}$ values for the two waves are decreasing by about $30/n\alpha$ mV ($15/\alpha$ mV, as $n = 2$) for each decade of increase in scan rate. The angular coefficient (θ)

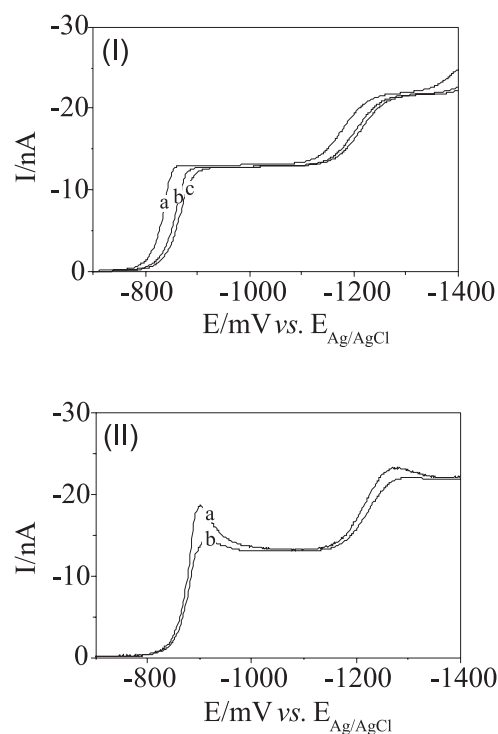


Figure 3. LSV curves for DIP 0.50 mmol L $^{-1}$ in 0.10 mol L $^{-1}$ phosphate buffer solution (pH 3.0), using a Hg-ME. ν (I): (a) 2; (b) 10; (c) 20 mV s $^{-1}$. (II) (a) 100; (b) 200 mV s $^{-1}$.

Table 1. Electrochemical parameters obtained for the voltammetric DIP 0.50 mmol L⁻¹ reduction in 0.10 mol L⁻¹ phosphate buffer solution (pH 3), Hg-UME. (1) First wave. (2) Second wave

ν (mV s ⁻¹)	$E_{1/2}$ (1) (mV)	I_d (1) (nA)	θ (1) (mV)	$n\alpha$ (1)	$E_{1/2}$ (2) (mV)	I_d (2) (nA)	θ (2) (mV)	$n\alpha$ (2)
2	-822	-12.77	40	1.48	-1181	-8.67	46	1.28
10	-839	-12.65	39	1.51	-1205	-8.68	45	1.31
20	-847	-12.69	40	1.48	-1213	-8.69	46	1.28
100	-863	-14.15	43	1.37	-1224	-8.90	44	1.34
200	-868	-18.45	42	1.40	-1235	-10.11	44	1.34

for the first and second waves is also indicative of the irreversibility of DIP electroreduction.

With the aim of comparing Hg-UME results, the effect of scan rate was also studied using a conventional HMDE and the cyclic voltammetric curves were obtained in the range of 10 mV s⁻¹ to 10 V s⁻¹. This extended range was used to verify the occurrence of a homogeneous chemical reaction coupled to the electrode process and to confirm the irreversibility of the electrode reaction. Figure 4(II) shows that below 10 V s⁻¹ there is no registered current peak in the reverse scan, diagnosing the irreversibility of the system in this time window. Also in CV experiments the peak potentials shift to more cathodic values, about 30/n α mV by decade of scan rate, as expected for an irreversible process.

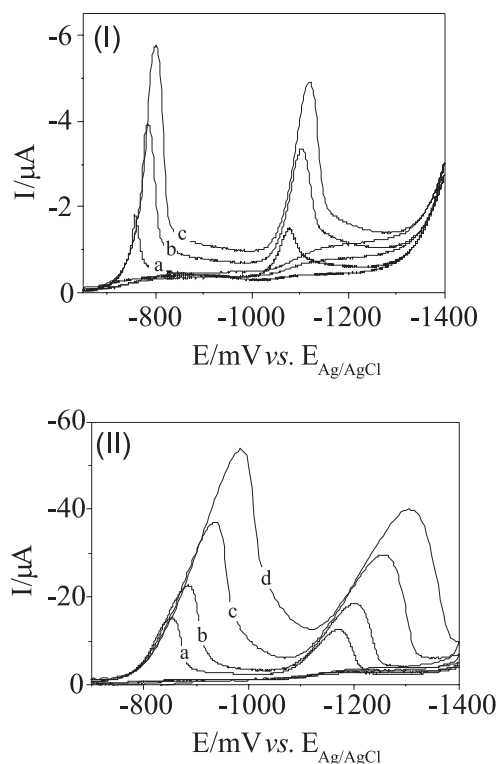


Figure 4. CV curves for 0.10 mmol L⁻¹ DIP in 0.10 mol L⁻¹ phosphate buffer solution (pH 3.0), using a HMDE (A = 0.01 cm²). ν (I): (a) 10; (b) 20; (c) 200 mV s⁻¹. (II) (a) 1; (b) 2; (c) 5; (d) 10 V s⁻¹.

The obtained results concerning to the irreversibility of DIP electroreduction agree with those obtained in Zeng studies,¹⁷ but differ from Tunçel.¹⁶ This difference can be attributed to the minimized effects of adsorption products in polarography, since the drop always change, implying constantly surface renew, and thus the irreversibility caused by adsorption products is negligible.

The predominating kind of mass transport control in CV experiments could be known by log(I) vs. log(ν) curves. According to the literature,²⁴ the angular coefficient of these curves for a diffusional process should be equal to 0.50, being unitary for an adsorption controlled process. Intermediate values are indicative of a mixed control of these two processes. The angular coefficients for the two reductions peak ($\theta_1 = 0.54$, $R_1 = 0.9992$ and $\theta_2 = 0.56$, $R_2 = 0.9993$) reveal that the diffusion mass transport to the electrode surface controls the reaction. The nature of the mass transport control is confirmed by the linearity of I_p vs. $\nu^{1/2}$ curves ($R_1 = 0.9989$ and $R_2 = 0.9991$), which is also in according with Zeng studies.¹⁷

DIP concentration vs. diffusion current

The relation between DIP concentration and the registered diffusion current was measured in the range of 0.50 x 10⁻⁴ to 4.80 x 10⁻⁴ mol L⁻¹ in phosphate buffer solution (pH 3.0). Figure 5(I) shows LSV curves for different DIP concentrations obtained by using Hg-ME. In the insert of the Figure 5(I) the I_d vs. C_{DIP} curves for both waves are presented.

The I_d vs. C_{DIP} curves (insert of Figure 5(I)) show that the linearity is obeyed for the limiting current measured after the current maximum in all studied concentration ranges, with good linearity (First wave, $R = 0.9976$ and second wave, $R = 0.9979$), as can be expected for a diffusion-controlled process.

Experiments for varying DIP concentration were also carried out using the HMDE in the same conditions as for Hg-ME (Figure 5(II)) and the peak currents (I_p) plotted against concentration are showed in the insert of Figure 5(II). It can be seen that probably because of the accuracy

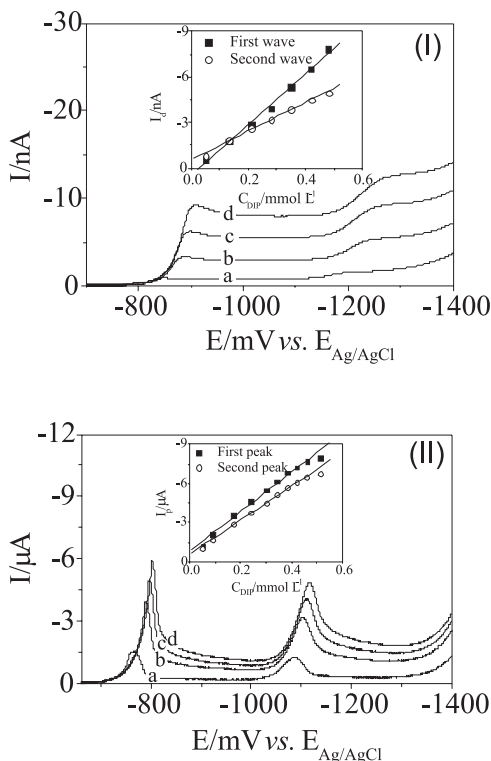


Figure 5. LSV curves for DIP in 0.10 mol L⁻¹ phosphate buffer solutions (pH 3.0). (I) Working electrode: Hg-ME. (II) Working electrode: HMDE (A = 0.01 cm²). Concentrations: (a) 0.05; (b) 0.21; (c) 0.35; (d) 0.48 mmol L⁻¹. n = 50 mV s⁻¹. Insert: (I) I_d vs. C_{DIP} curves for: (■) first wave (R = 0.9976); (○) second wave (R = 0.9979). (II) I_p vs. C_{DIP} for: (■) first peak (R = 0.9988); (○) second peak (R = 0.9974).

of DIP adsorption on the electrode surface, for concentrations above 0.42 mmol L⁻¹, the I_p for both peaks begins failing to seek the linearity with the increase in DIP concentration. The shape of the first peak, like the maximum on the top of the first Hg-ME wave resembles a first order polarographic maximum that suggests the occurrence of an adsorption process.

Effect of acidity

Due to the low solubility of DIP in neutral media (15.0 μmol L⁻¹)²⁵ and the low sensitivity of LSV technique, an investigation was carried out in solution of pH ranging from 1.5 to 4.5, where the solubility of the compound increases. Linear sweep voltammograms presented in Figure 6 show that when the pH is increased from 1.5 to 4.5, the first half-wave potentials shift to more cathodic values by ca. 39 mV for the first wave and by ca. 32 mV for the second wave by unity of pH, revealing that the two electrode reactions are coupled with the consumption of protons.

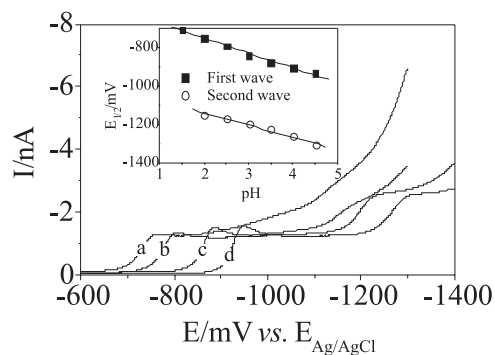


Figure 6. LSV curves for DIP 0.10 mmol L⁻¹ in 0.10 mol L⁻¹ phosphate buffer solutions. Working electrode: Hg-ME. pH values: (a) 1.5; (b) 2.0; (c) 3.0; (d) 4.0. Insert: E_{1/2} vs. pH curves for: (■) first wave (R = 0.9942; dE_{1/2}/dpH = 82 mV); (○) second wave (R = 0.9906; dE_{1/2}/dpH = 64 mV).

In the insert of Figure 6, E_{1/2} vs. pH curves were showed for both waves resulting in good linearity (First wave, R = 0.9942 and second wave, R = 0.9906). Using the angular coefficient of these curves (First wave, dE/dpH = 82 mV and second wave, dE/dpH = 64 mV), the number of protons (P) consumed in the two reduction steps was calculated from equation (1). By this way, it is possible to conclude that both reactions occur with the consumption of two protons (First step, P = 2.0 and second step, P = 1.6).

$$dE_{1/2}/dpH = -59P/n\alpha \quad (1)$$

The nα values (First step, nα = 1.43; Second step, nα = 1.52) were calculated as described above, using the angular coefficient (θ) obtained from log(I_d-I)/I vs. E curves at different pH values.

The fractional number of protons for the second wave means that the irreversibility of this wave changes in the pH range studied, which can be observed by the shape of the curves for this step as the pH increases, justifying the lower nα and P values obtained.

Determination of DIP diffusion coefficient

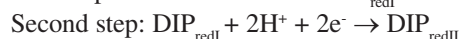
The apparent DIP diffusion coefficient was estimated in phosphate buffer (pH 3.0) from the limiting current concerning to the first reduction step, and was compared with the limiting diffusion current observed for hexaminrutenium (III) chloride, as a standard, under the same experimental conditions.

As the Hg-ME geometry is already known, the diffusion coefficient for hexaminrutenium was calculated, from equation (2), where r_h is the radius of the Hg-ME hemispheric and the other terms have their usual meaning. Using this equation, the diffusion coefficient for

hexaminrutenium is equal to $5.99 \times 10^{-6} \text{ cm}^2 \text{ s}^{-1}$. In the literature,²⁰ the diffusion coefficient of this standard, determined under the same conditions, is expected as being $6.0 \times 10^{-6} \text{ cm}^2 \text{ s}^{-1}$, which is in perfect agreement with experimental data. Thus, with the same conditions, it was possible to estimate DIP diffusion coefficient as being equal to $2.04 \times 10^{-5} \text{ cm}^2 \text{ s}^{-1}$.

$$I_d = 2\pi n F D C r_h \quad (2)$$

From voltametric experiments, we have attributed formally the following equations for electroreduction of DIP:



Conclusions

The electroreduction of DIP, in phosphate buffer solution (pH 3.0), with a mercury coated platinum microelectrode (Hg-ME), revealed that the reaction occurs in two irreversible steps of two electrons each, with the consumption of two protons per step. The apparent DIP diffusion coefficient was calculated ($2.04 \times 10^{-5} \text{ cm}^2 \text{ s}^{-1}$) through the measuring of the limiting Hg-ME current concerning to the first reduction step. Results obtained with Hg-ME are in agreement with those obtained using a conventional hanging mercury drop electrode (HMDE). For analytical proposes, Hg-ME can be applied for detection of DIP in medicines and in biological fluids with good promises, due to the low detection limits that can be reached with electroanalytical pulse techniques and the facility of Hg-ME surface renew. Works in our laboratory are in course dealing with the determination of DIP in medicines with Hg-ME and HMDE using square wave voltammetry.

Acknowledgments

The authors are indebted to FAPESP, CAPES and CNPq.

References

- Darbar, D.; Gillespie, N.; Main, G.; Bridges, A.B.; Pringle, N.S.J.; Mcneill, G.P.; *Amer. J. Cardiol.* **1996**, *78*, 736.
- Borges, C.P.F.; Borissevitch, I.E.; Tabak, M.; *J. Lumin.* **1995**, *65*, 105.
- De La Cruz, J.P.; Carrasco, T.; Ortega, G.; Sánchez de la Cuesta, F.; *Lipids* **1992**, *27*, 192.
- Iuliano, L.; Pedersen, J.Z.; Rotilio, G.; Ferro, D.; Violi, F.; *Free Rad. Biol. Med.* **1995**, *18*, 239.
- Castilho, M.; Almeida, L.E.; Mazo, L.H.; Tabak, M.; *Anal. Chim. Acta* **1998**, *375*, 223.
- Castilho, M.; Almeida, L.E.; Tabak, M.; Mazo, L.H.; *Electrochim. Acta* **2000**, *46*, 67.
- Castilho, M.; Almeida, L.E.; Tabak, M.; Mazo L.H.; *J. Braz. Chem. Soc.* **2000**, *11*, 148.
- Curtin, N.J.; Turner, D.P.; *Euro. J. Cancer* **1999**, *35*, 1020.
- Labianca, R.; Pessi, A.; Facendola, G.; Pirovano, M.; Luporini, G.; *Euro. J. Cancer* **1996**, *32A*, suppl. 5, S7.
- Wang, Z.; Zhang, H.; Zhou, S.; *Talanta* **1997**, *44*, 621.
- Pulgarín, J.A.M.; Molina, A.A.; López, P.F.; *Analyst* **1997**, *119*, 253.
- Issa, A.S.; Mahrous, M.S.; Salam, M.A.; Soliman, N.; *Talanta* **1987**, *34*, 670.
- Stern, J.M.; *J. Chromatogr.* **1979**, *164*, 487.
- Heyob, M.B.; Merlin, J.L.; Pons, L.; Calco, M.; Weber, B.; *J. Liq. Chromatogr.* **1994**, *17*, 1837.
- Pulgarín, J.A. M.; Molina, A.A.; López, P.F.; *Anal. Biochem.* **1997**, *245*, 8.
- Tunçel, M.; Yazan, Y.; Dogrukol, D.; Atkosar, Z.; *Anal. Lett.* **1991**, *24*, 1837.
- Zeng, X.; Lin, S.; Hu, N.; *Talanta* **1993**, *40*, 1183.
- Correia, A.N.; Mascaro, L.H.; Machado, S.A.S.; Mazo, L.H.; Avaca, L.A.; *Quim. Nova* **1995**, *18*, 475.
- Silva, S.M.; Alves, C.R.; Correia, A.N.; Martins, R.M.; Nobre, A.L.R.; Machado, S.A.S.; Mazo, L.H.; Avaca, L.A.; *Quim. Nova* **1998**, *21*, 78.
- Wehmeyer, K.R.; Wightman, R.M.; *Anal. Chem.* **1985**, *57*, 1989.
- Colyer, C.L.; Luscombe, D.; Oldham, K.B.; *J. Electroanal. Chem.* **1990**, *283*, 379.
- Stojek, Z.; Osteryoung, J.; *Anal. Chem.* **1989**, *61*, 1305.
- Machado, S.A.S.; Mazo, L.H.; Avaca, L.A.; *J. Braz. Chem. Soc.* **1992**, *3*, 89.
- Gosser Junior, G.K.; *Cyclic Voltammetry: Simulation and Analysis of Reaction Mechanisms*, VCHP: New York, 1993.
- Borissevitch, I. E.; Borges, C.P.F.; Borissevitch, G.P.; Yushmanov, V.E.; Louro, S.R.W.; Tabak, M.; *Z. Naturforsch.* **1996**, *51C*, 578.

Received: April 17, 2003

Published on the web: May 10, 2004

FAPESP helped in meeting the publication costs of this article.